The electrochemical behavior of flavin adenine dinucleotide in neutral solutions

V. I. BIRSS,[1] H. ELZANOWSKA, AND R. A. TURNER
Department of Chemistry, University of Calgary, Calgary, Alta., Canda T2N 1N4

Received February 20, 1987[2]

V. I. BIRSS, H. ELZANOWSKA, and R. A. TURNER. Can. J. Chem. **66**, 86 (1988).

A detailed investigation of the electrochemical behavior of flavin adenine dinucleotide (FAD) in neutral solutions has been carried out at Hg and glassy carbon electrodes. At FAD concentrations of about 10^{-4} *M*, cyclic voltammetry (CV) shows a pair of anodic and cathodic peaks having a peak separation at low sweep rates indicative of a two-electron transfer process and yielding a formal redox potential for FAD of -0.206 ± 0.003 V vs. NHE at pH 7. Evidence for FAD adsorption was obtained in experiments at high sweep rates, from the effect of time of exposure of the electrode surface to FAD in solution and from the effect of the potential limits on the cyclic voltammetric response. The process of FAD adsorption was studied in detail in dilute FAD solutions (ca 10^{-6} *M*) using a hanging mercury drop electrode and the techniques of CV and ac voltammetry. Three distinct stages of FAD adsorption were observed and a model of the orientation of FAD on the electrode surface as a function of time and potential is presented. In addition, the kinetics of oxidation and reduction of adsorbed FAD was studied for each of the stages of FAD deposition, and a surface standard rate constant of ca. 40 s^{-1} was obtained for Stages II and III of FAD adsorption.

V. I. BIRSS, H. ELZANOWSKA et R. A. TURNER. Can. J. Chem. **66**, 86 (1988).

Opérant en solutions neutres et à des électrodes de Hg ainsi que de verre, on a réalisé une étude détaillée du comportement électrochimique du dinucléotide de la flavine et de l'adénine (DFA). A des concentrations de DFA d'environ 10^{-4}, la voltamétrie cyclique (VC) présente une paire de pics anodique et cathodique qui possèdent, à des vitesses de balayage lentes, une séparation entre les pics qui suggère qu'il s'agit d'un processus de transfert de deux électrons et qui, à un pH de 7, fournit pour le DFA un potentiel redox formel de $-0{,}206 \pm 0{,}003$ V vs. NHE. On a obtenu des indications relatives à l'adsorption du DFA au cours d'expériences à des vitesses élevées de balayage; ces indications découlent de l'effet du temps d'exposition de la surface de l'électrode au DFA en solution ainsi que de l'effet des limites de potentiel sur la réponse voltamétrique cyclique. On a étudié en détail le processus d'adsorption du DFA en solutions diluées (environ 10^{-6} *M*) en utilisant un électrode à goutte tombante de mercure ainsi que les techniques de VC et de voltamétrie à c.a. On a observé trois stages distincts d'adsorption du DFA et on présente un modèle de l'orientation du DFA sur la surface de l'électrode en fonction du temps et du potentiel. De plus, on a étudié la cinétique de l'oxydation et de la réduction du DFA adsorbé pour chacun des stages de la déposition du DFA; on a obtenu une constante de vitesse standard d'environ 40 s^{-1} pour les stages II et III de l'adsorption du DFA.

[Traduit par la revue]

Introduction

The redox-active flavoproteins play a particularly important biological role in the electron transfer reactions of all living systems. These proteins utilize the cofactor flavin adenine dinucleotide (FAD) to dehydrogenate (oxidize) pyridine nucleotides and hydrogenate (reduce) the cytochromes (1, 2). This valuable cofactor, which is derived from riboflavin (RF) (Vitamin B_2), is unique in that, depending on the conditions, it can undergo either two separate one-electron transfer reactions or one essentially simultaneous two-electron transfer reaction. The flavin coenzymes occur in a variety of proteins and interface between organic oxidation and reduction reactions, which are usually two-electron processes, and electron transfer reactions to/from metal centers, often requiring only one electron. The two one-electron reactions are shown below involving a proton and producing neutral molecules (Fl = flavin).

[1] $\mathrm{Fl} + \mathrm{H}^+ + \mathrm{e}^- \rightleftharpoons \mathrm{FlH}$

[2] $\mathrm{FlH} + \mathrm{H}^+ + \mathrm{e}^- \rightleftharpoons \mathrm{FlH_2}$

All flavins share the isoalloxazine moiety, which is the electroactive part of the molecule (Fig. 1). Attached to this ring system is another group, depicted as R in Fig. 1, which aids in apoprotein–cofactor binding and specificity (1, 2). The isoalloxazine ring system can exist in an oxidized form (quinone), the radical semiquinone form, after the acceptance of the first electron, and the reduced hydroquinone form, after a second electron transfer. Therefore, all compounds derived from flavin, e.g., lumiflavin (LF), riboflavin, flavin mononucleotide (FMN), and FAD, which vary only in the nature of the R group (Fig. 1), are expected to have similar formal potentials to that of the isoalloxazine ring system. It should also be noted that depending on the solution pH, each of these species can exist in either neutral or ionic forms (1).

In biological systems, the factors which govern the mechanism of FAD reduction and oxidation, as well as its redox potential, are related to the microenvironment of the cofactor–apoprotein interaction site. For example, steric hindrance, solution pH, and ionic strength all give rise to unique microenvironments (2, 3), and therefore may affect the redox potential of the flavin.

It is also known that, in solution, the oxidized flavins are expected to have a planar structure, while the reduced flavin resembles a butterfly in conformation (2), with atoms 1 to 5 and 10, and 5 to 9 and 10 (Fig. 1) constituting two planes or wings intersecting the N(5)—N(10) axis, with a dihedral angle of 21° (4). Therefore, enforced flattening of the reduced flavin should increase its reducing power, and conversely, enhanced bending should increase the oxidizing power. Selectivity for a one- or two-electron reaction could conceivably be assisted in this manner (4). This may occur in the protein and could perhaps also occur at the surface of an electrode.

The electrochemical behavior of the flavins, particularly of RF, has been studied at Hg electrodes, primarily with the use of dc and ac polarographic and also chronopotentiometric methods (5–9). It has been reported that in acidic solutions, both the oxidized and the reduced forms of RF are strongly adsorbed on a Hg surface (5, 6, 10). One monolayer of oxidized RF oriented parallel to the electrode surface and two layers (a bilayer) of the reduced RF ($\mathrm{RFH_2}$) are thought to adsorb (8, 9). Despite the

[1]To whom correspondence should be addressed.
[2]Revision received September 14, 1987.

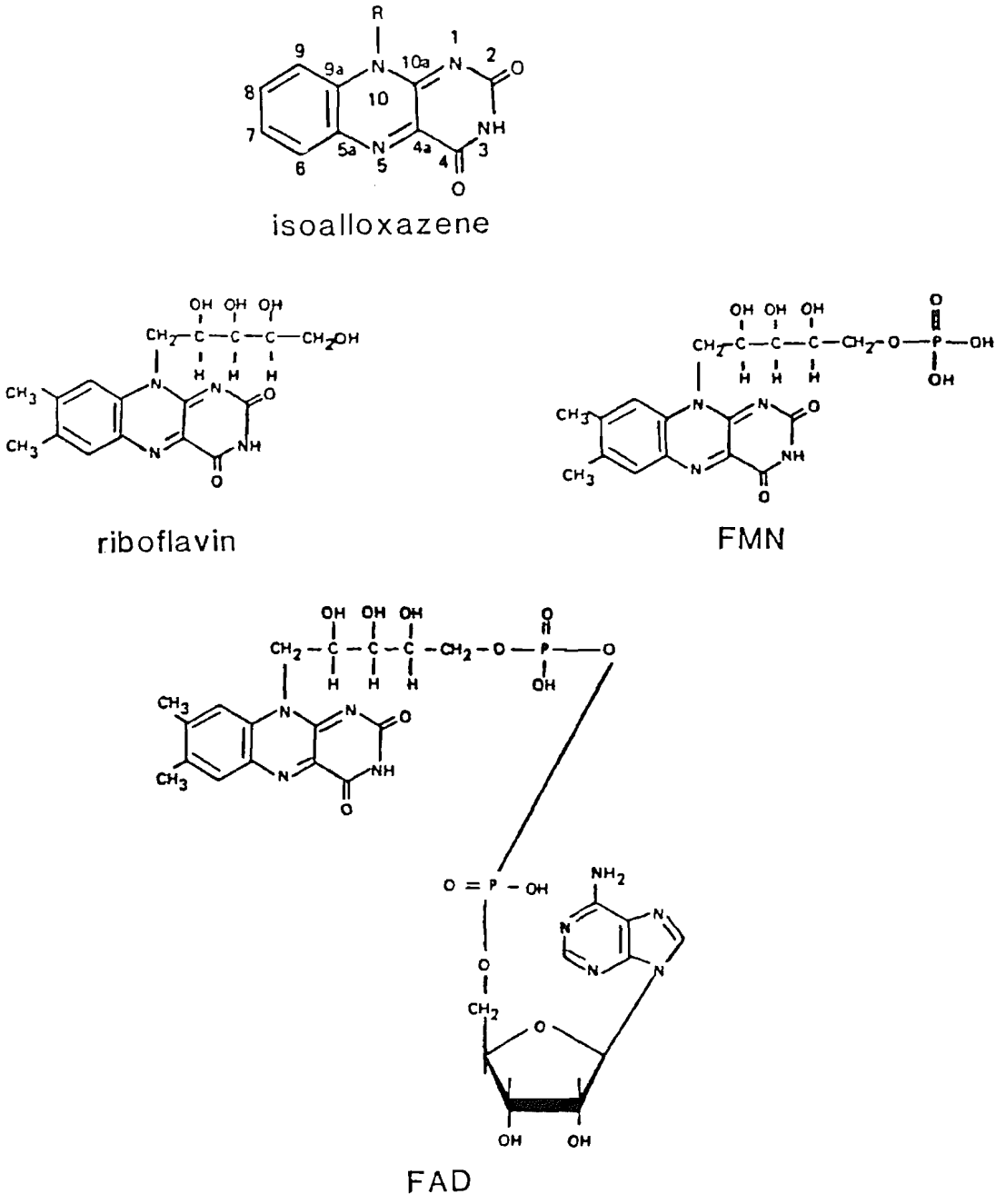

FIG. 1. Structure of isoalloxazine moiety and of the R groups for RF, FMN, and FAD.

presence of these adsorbed layers, the reduction of RF from solution was found to occur via a reversible two-electron transfer reaction (9).

A study of the adsorption behavior of FMN at Hg electrodes in acid solutions has also been reported (11). As in the case of RF, strong adsorption of both the oxidized and reduced forms of FMN are observed electrochemically. Also, a bilayer (1.2×10^{-10} mol/cm^2) of the reduced form is presumed to be present, while only a single layer (0.6×10^{-10} mol/cm^2) of the oxidized form of FMN is found to adsorb at the Hg electrode (11).

In a more recent work (12), it was shown that both the oxidized and the reduced forms of FMN are strongly adsorbed at a Hg drop electrode in buffered solutions of pH 4.9 and 6.9. The quantity of adsorbed FMN, as measured by cyclic voltammetry, was estimated to be in the range of 7 to 9×10^{-11} mol/cm^2, close to the predicted amount of FMN (7.5×10^{-11} mol/cm^2) having the isoalloxazine ring system parallel to the electrode surface (12).

The same authors also carried out a similar study using a Hg electrode in dilute FAD solutions buffered to a pH of 6.9 (13), and again, both the oxidized and reduced forms of the flavin were found to be strongly adsorbed. In concentrated FAD solutions, another investigation (14), carried out over the entire range of pH, has dealt in detail with the mechanism of reduction of FAD in solution, but did not discuss FAD adsorption.

An area of current interest which is of relevance to studies of flavin adsorption involves the attachment of various important redox materials to electrode surfaces, producing chemically modified electrodes. This has been carried out recently for FAD, which has been successfully attached to various graphite

and carbon electrode surfaces (15–20). At glassy carbon electrodes, a single layer of FAD can be attached, while at porous graphite electrodes, up to 50 to 100 monolayers of FAD have apparently been adsorbed (18, 20). However, it appears that the roughness factor of these porous graphite electrodes was not taken into account in estimating the number of FAD layers adsorbed, and therefore, it is likely that only ca. one layer is also deposited on these electrodes. In all of this work at carbon electrodes, it was found that glucose oxidase activity in solution could be restored with the use of the FAD-coated electrode. FAD has also been attached to an indium – tin oxide electrode via the adenine amino group (20).

While most of the papers described above have reported that the flavins do indeed adsorb at electrode surfaces, none of them has investigated the actual mechanism of build-up of adsorbed flavin layers or the kinetics of their oxidation and reduction. The present investigation has involved the use of cyclic voltammetry to study the oxidation and reduction of FAD at mercury electrodes in neutral solutions and to discover whether two separate one-electron transfer steps can be distinguished at rapid sweep rates. Also, a detailed examination of the process of FAD adsorption, the oxidation and reduction of adsorbed FAD and layer reorientation has been carried out using cyclic voltammetry (CV) and alternating current (ac) voltammetry.

Experimental

(a) Equipment

Standard three-electrode potentiostatic circuitry was employed, utilizing either a PAR 173 potentiostat and a PAR 175 universal programmer, or a PAR 273 digital potentiostat/function generator for the cyclic voltammetry experiments. I/E curves were usually plotted on a HP 7044A X/Y recorder at slow potential sweep rates (s), and on either a Nicolet 3091 digital oscilloscope or a HP 7090A digital recorder at s greater than about 200 mV/s.

The ac voltammetry experiments were carried out using a PAR 273 potentiostat in conjunction with a PAR 5206 Lock-in Amplifier. For most experiments, a voltage amplitude of 5 mV, a frequency of 329 Hz, and phase angles of either 0° or 90° were employed.

(b) Electrodes

The working electrodes (WE) utilized in this work were either a Hg pool electrode, a PAR 303A HMDE, or a glassy carbon electrode. The HMDE was utilized only on the medium drop size setting, producing a drop having a surface area of 1.3×10^{-2} cm^2. The Hg pool electrode, contacted with a Pt wire, had a surface area of 2 cm^2. The surface areas were determined by measuring the minimum capacity in a flavin-free buffer solution and comparison with the reported double layer capacity minimum of 15.4 μF/cm^2 for Hg in phosphate solutions (21). In this paper, all current and charge densities are given with respect to the electrode areas measured by this method.

The glassy carbon (GC) electrode (5 mm radius) consisted of a GC disc placed into the end of some shrinkable Teflon tubing, which was then heated, leaving only the end of the disc exposed to the solution. Electrical contact was made at the back of the GC disc by a Ni wire embedded into a drop of Hg. The GC electrode surface was prepared by polishing with γ alumina, followed by ultrasonic cleaning in acetone for about 1 min and then a thorough rinse with distilled water.

The counter electrode (CE) used in these experiments was either a Pt gauze or Pt wire electrode. The reference electrodes (RE) were either a Ag/AgCl electrode or an SCE. All potentials are given vs. the NHE in this paper.

(c) Cells and solutions

All experiments were carried out in either a two compartment cell or in the standard polarographic cell used with the PAR 303A HMDE. Both cells were constructed so that the cell solution could be thoroughly deoxygenated by bubbling argon or nitrogen either through the solution or passing it above the solution during the experimental runs.

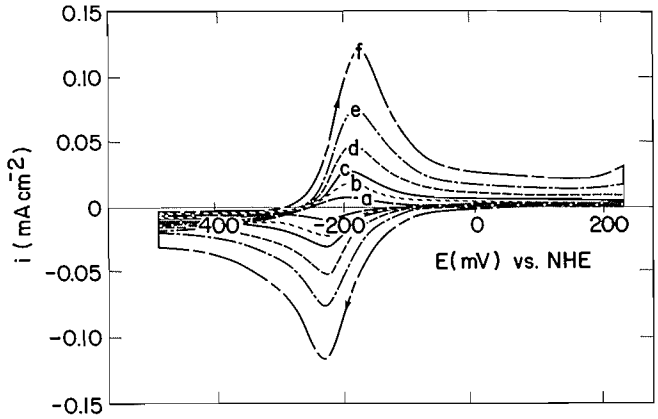

FIG. 2. Cyclic voltammograms obtained at a Hg pool electrode in 1.1×10^{-4} M FAD solution (pH = 7). s = 2 (a), 10 (b), 20 (c), 50 (d), 100 (e), and 200 (f) mV/s.

The experiments were carried out in buffered (sodium phosphate or potassium hydrogen phthalate) solutions. FAD was obtained as its sodium salt from Sigma Chemicals Co. The flavin solution concentrations ranged from about 2×10^{-6} to 1×10^{-4} M. All chemicals utilized were of reagent grade and all water was thrice distilled. All experiments were carried out at room temperature.

Results and discussion

(a) General electrochemical behavior of FAD at Hg electrodes

Initial experiments were carried out with the use of cyclic voltammetry (CV) to establish whether a single two-electron or two one-electron transfer steps would be observed for FAD reduction and oxidation over a wide range of s. A Hg pool electrode was used for these early experiments (at sweep rates less than or equal to ca. 500 mV/s), primarily as it was anticipated that in the subsequent adsorption studies, it would be desirable to transfer the Hg electrode from one solution to another and it was considered that a Hg pool electrode would facilitate this process.

Figure 2 shows a family of CVs for a range of s from 2 to 200 mV/s and a FAD concentration of 1.1×10^{-4} M (pH = 7). This rather high FAD concentration was selected so that the diffusion currents would be significantly larger than the current due to the reaction of adsorbed FAD. However, despite this, the peaks are somewhat non-ideal in shape, having a greater peak separation and being wider at half-height than theoretically predicted (22).

Figure 3a (□) shows that at low s, the difference in the anodic and cathodic peak potentials (ΔE_p) is constant at about 35 mV for the Hg pool electrode. This is somewhat larger than the expected value for a reversible two-electron transfer reaction, $57/z$ mV, where z is the number of electrons transferred in the process (2). At sweep rates greater than about 20 mV/s, the peak separation begins to increase, as is predicted for the onset of kinetic irreversibility.

When the peak current density (i_p) is plotted vs. $s^{1/2}$ (Fig. 3b), a linear relationship is observed up to a sweep rate of about 20 mV/s. However, rather than observing a decrease in the slope of this plot at high s, as might have been expected when a diffusion-controlled process becomes irreversible (22), the slope of the plot increases. This is indicative of the presence of adsorbed flavin, as the current due to the oxidation and reduction of adsorbed species is expected to vary linearly with s, rather than with $s^{1/2}$ (22). This result implies that the increased peak separation at higher sweep rates, shown in Fig. 3a, is

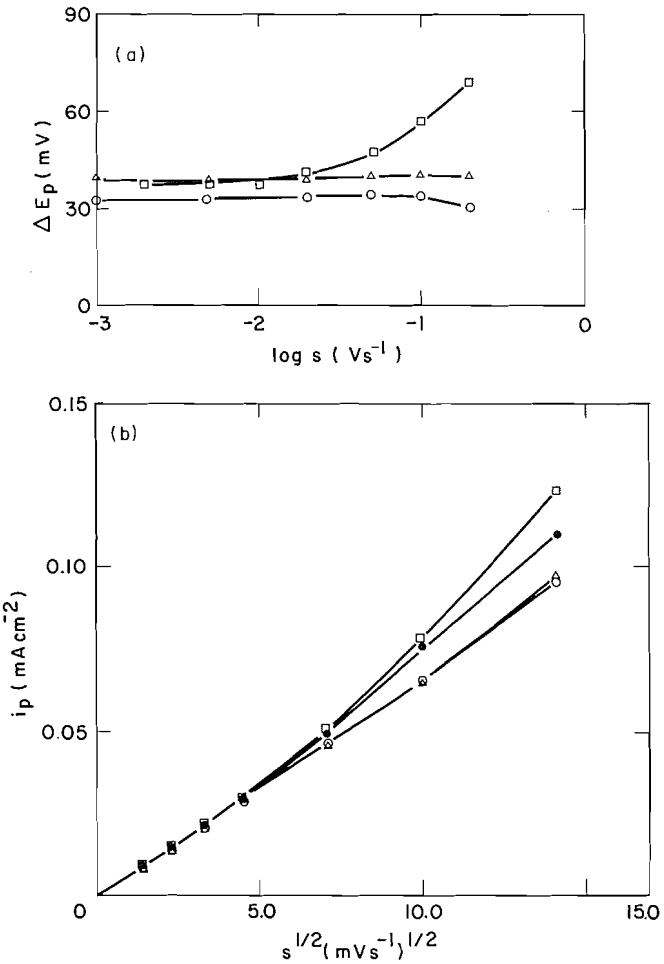

FIG. 3. (*a*) ΔE_p vs. log s; 1.1×10^{-4} *M* FAD solution (pH = 7), using a Hg pool electrode (□) or a HMDE, where (○) represents the "first scan" of potential and (△) scans nos. 2, 3, and 4. (*b*) The dependence of $i_{p,c}$ (●, ○) and $i_{p,a}$ (□, △) on $s^{1/2}$ for 1.1×10^{-4} *M* FAD solution (pH = 7) at a Hg pool electrode (●, □) and the HMDE (○, △).

related to contributions to the current peak from the reaction of both adsorbed flavin and flavin molecules diffusing to the surface from the solution. Therefore, a simple estimation of the rate constant for the reaction cannot be obtained from the results of Fig. 3. It can be seen in Fig. 3*b* that the anodic peak is influenced more by adsorption than is the cathodic peak. This is in agreement with the findings (reported below) that the adsorption peaks are centered at a somewhat more positive potential than the diffusion peaks (Table 1).

It should be noted that even at sweep rates greater than 500 mV/s, no evidence for the splitting of the main FAD reduction and oxidation peaks into those for the individual one-electron transfer steps was observed, notwithstanding the difficulty in avoiding the current response to adsorbed FAD at high sweep rates. This is consistent with the reported E^0 values for reactions [1] and [2], −240 and −130 mV, respectively (23), measured by the coulometric titration of flavin bound to a benzoate substrate. Anderson (24) utilized pulse radiolysis and obtained E^0 values of −314 and −124 mV for the two reactions. These values indicate that as soon as the first electron is transferred in the reduction process, the second should pass immediately thereafter. As stated earlier, in biological systems, it is possible that binding and local environment effects could

TABLE 1. Characteristics of FAD adsorption peaks (HMDE, 1.8×10^{-6} *M* FAD, pH = 7)

Stage	q (μC cm^{-2})	E_f' (mV vs. NHE)*	ΔE_p (mV)†
I	8–9	−189	16–20
II	12.5–13	−202	8–10
III	13–13.5	−189	14–17

*Determined as the potential midway between the anodic and cathodic peak (cf. with E_f = ca. −206 mV).
†Measured at s = 100 mV/s.

cause the second step to become more difficult than the first, or the first to become more facile, so that the two one-electron steps could become more readily separated (23). The observation of a two-electron transfer process has been reported previously for FAD (14, 25–27), although two overlapping one-electron steps have sometimes been reported for RF (28), FMN (29, 30), and for FAD (14), particularly in acid solutions. It has also been reported that flavins coordinated to particular metal centers, e.g. $Ru^{2+/3+}$, undergo electron transfer in discreet one-electron steps, rather than in one two-electron step, in both aqueous and non-aqueous solutions, e.g. DMF (31–33).

Efforts were made to determine the formal potential, E_f, of the reaction from CVs such as those shown in Fig. 2. The potential midway between the anodic and cathodic peaks, −0.208 ± 0.002 V vs. NHE, was taken as E_f at pH = 7 at the Hg pool electrode. There are numerous values reported in the literature for this potential, e.g. −0.205 V (14), −0.210 V (26), −0.213 V (29), −0.219 V (34) etc. Our value is well within this range.

The strong adsorption of FAD at Hg electrodes has been demonstrated by replacing the FAD solution with buffer solution only and then monitoring the electrochemical response. A matching pair of peaks were observed in the same potential range as the diffusion peaks had been. These peaks were seen both when the Hg electrode was at open-circuit during the exchange of solutions as well as when potential control was maintained and the transfer of solutions was done in a flow-through cell. These peaks contain a charge equivalent to about one layer of adsorbed FAD (see below) and demonstrate conclusively the strong adsorption of both the oxidized and the reduced forms of FAD on the Hg surface.

It was also found that when the FAD solution was removed from the cell, the Hg was shaken/rinsed with water, and the pool electrode was replaced in the cell containing only the buffer solution, the small adsorption peaks were still present. The only absolute method for removing the adsorbed flavin was by washing the Hg electrode in HCl, after which only a small fraction of the adsorption peaks could still be seen. Very similar effects were seen with GC electrodes after exposure to FAD solutions. The only method by which the adsorbed FAD could be removed was by a mechanical polishing of the GC surface. These experiments indicate clearly why a simple kinetic analysis could not be carried out for the reduction and oxidation of FAD from solution at these Hg pool electrodes.

An interesting effect observed at the Hg pool electrode in phosphate buffered FAD solutions was that when the potential was extended to potentials more negative than about −0.800 V vs. NHE, a new pair of peaks was observed at ca. −0.85 V (Fig. 4). If the potential was held just negative of these peaks for several minutes, the next complete anodic run (Fig. 4) displayed a new peak on the positive side of the main FAD oxidation

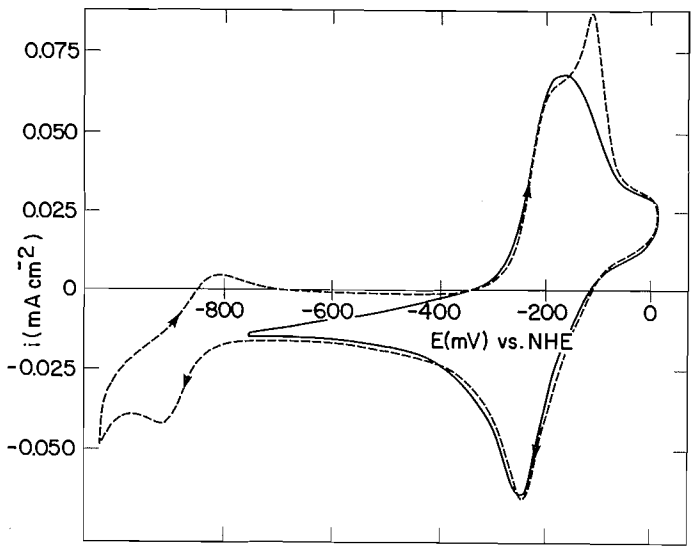

FIG. 4. Cyclic voltammogram at Hg pool electrode in 1×10^{-4} *M* FAD solution (pH = 7), s = 100 mV/s. The dashed line shows the influence of extended negative potential limit on anodic peak.

peak. This new peak was quite sharp and exceeded the anodic diffusion peak in magnitude. This was observed at both Hg and GC electrodes in this work. This is a similar effect to that reported for FMN at Hg electrodes in pH 1 solutions (11), in which an anodic "post-peak", considered to be due to $FMNH_2$ adsorption, splits to give a second, rather sharp post-peak at more positive potentials after time spent at potentials cathodic of the main reduction peak.

The behavior observed in Fig. 4 is therefore also likely to be indicative of FAD adsorption at the Hg pool electrodes. It will be shown below that it represents a reorientation within the underlying adsorbed FAD film. In the case of FMN (11), no small peaks such as those at negative potentials in Fig. 4 were reported.

It should be noted that at pH 4, neither the small peaks at ca. −0.85 V nor the new anodic spike are observed. It is probably significant that at pH 7, the anion form of both the semiquinone (FlH) and the hydroquinone (FlH_2) may be present in reasonable quantities, while at pH 4, all forms of FAD are neutral. Therefore, it is likely that the new anodic spike is related to reorientation of adsorbed negatively-charged FAD at negative potentials. It will be shown below that similar effects of holding the potential at the negative limit of the potential range are seen in the electrochemical response of adsorbed FAD. The small peaks at negative potentials in Fig. 4 will be shown below to be due to the capacitive change caused by the desorption and reorientation of FAD (see ac results below).

From the results presented above, it was concluded that the Hg pool electrode becomes covered with a strongly adsorbed FAD film which clearly influences the shape and position of the peaks observed by CV and which may influence the kinetics of the oxidation and reduction of FAD from solution. For these reasons, and also in order to produce a fresh, reproducible Hg electrode surface readily, all subsequent studies were carried out with the HMDE. The use of the HMDE also enabled a thorough study of the mechanism of the build-up of adsorbed FAD to be carried out.

(b) FAD electrochemistry at the HMDE

The CVs of FAD reduction and oxidation at the HMDE were generally similar to those in Fig. 2 for the Hg pool electrode. However, the extent of FAD adsorption could be more readily controlled by extruding a fresh Hg drop just before recording the CV, and comparing this result to those at later times. Figure 3*a* (○) shows ΔE_p as a function of the sweep rate for the first sweep at a fresh Hg drop as well as for later sweeps. A fresh Hg drop was extruded for the measurements at each sweep rate. For the first sweep at a fresh Hg drop, it can be seen that at sweep rates less than about 100 mV/s, ΔE_p is about 31 mV, close to the theoretically predicted peak separation of 28.5 mV (22). However, for the first sweep at sweep rates greater than 100 mV/s, a more ideal peak separation (29 mV) was observed, indicating that the electron transfer reaction is relatively rapid. It also indicates the probable influence of adsorption at low s (long times). This point is discussed further below.

These results indicate that FAD adsorption is a fast process at this high FAD concentration, causing an increased peak separation at low sweep rates. Only at high sweep rates, when little time is available for adsorption to occur, is the peak separation more ideal. The peak separation in the subsequent few sweeps at low s (Fig. 3*a*, △) is more similar to that at the Hg pool electrode, while at high s, the peak separation is smaller as less time has elapsed in the experiment and less FAD has adsorbed.

Figure 3*b* (○, △) also shows that less FAD is adsorbed at a Hg drop electrode in the first few sweeps of potential than at the Hg pool electrode, which remains exposed to the FAD solution for the duration of the experiment. This is seen by the fact that the $i_p/s^{1/2}$ relationship remains essentially linear, even at high s. In comparison, the results at the pool electrode in Fig. 3*b* (□, ●) show a significant deviation towards a linear i_p/s relationship at high s, indicative of a greater extent of current response from adsorbed FAD.

The formal potential of FAD reduction/oxidation, E_f, determined from these results at the HMDE, is −0.205 ± 0.002 V vs. NHE, again within the reported range of potentials for this reaction. It should be noted that by using the "first sweep" results at greater than ca. 100 mV/s at a freshly extruded Hg drop, it is likely that the potential is not influenced significantly by adsorption effects. Much of the older literature, e.g. ref. 29, shows non-ideal polarographic waves and has reported formal potentials from these waves. These potentials are likely to be more negative than those at a fresh Hg surface, when adsorption effects can be minimized.

(c) FAD adsorption at the HMDE in pH = 7 solutions

The study of the adsorption of FAD has been carried out in dilute FAD solutions (less than 5×10^{-6} *M*) and at relatively high s (greater than 100 mV/s). The purpose of this was to enhance the FAD adsorption currents relative to the diffusion controlled currents. The HMDE was used in all of this work because a fresh reproducible Hg surface could be produced at controlled intervals of time.

(i) General electrochemical behavior

The gradual build-up with time of adsorbed FAD at a fresh HMDE surface has been monitored using both CV and the out-of-phase (ϕ = 90°) "capacitive" current response to an ac signal. Figure 5*a* shows the ac response of the HMDE, first in the phosphate buffer supporting electrolyte solution only, with no FAD added, and then in a 1.8×10^{-6} *M* FAD solution in the buffer solution at s = 5 mV/s in the range of voltage between −0.650 and +0.250 V vs. NHE. The ac response is seen to reach a steady-state after the second scan. Figure 5*b* shows the analogous experiment, starting with a fresh Hg drop, using CV and s = 100 mV/s. The progression of time of cycling is

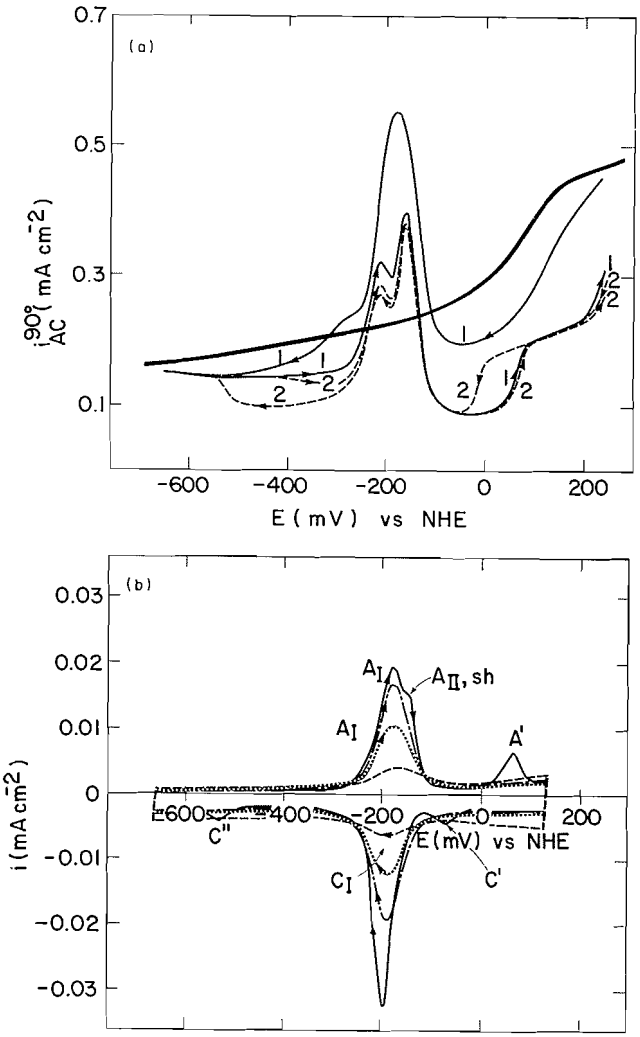

FIG. 5. Adsorption of FAD (Stages I and II) at fresh HMDE; 1.8×10^{-6} *M* FAD solution (pH = 7, 0.08 *M* phosphate buffer). (*a*) ac voltammograms where ΔE = 5 mV, ν = 329 Hz, s = 5 mV/s. (—) buffer solution only (no FAD); (—) first sweep in FAD solution (curve 1); (---) second sweep in FAD solution (curve 2). Note the "capacitance pit" between −0.55 V and +0.05 V. (*b*) Cyclic voltammograms in FAD solution; s = 100 mV/s. (---) sweep no. 1; (···) sweep no. 8; (-·-) sweep no. 16; (—) sweep no. 21. Note that peaks A′, C′, and C″ are related to the sudden changes of double layer capacitance seen in Fig. 5*a*.

indicated by the number of each of the runs (each run is equivalent to 16 s), given in the figure caption. It should be noted that because of the different sweep rates used in the ac and CV experiments, the time which elapses in one complete ac cycle is about 20 times that in one CV cycle.

In Fig. 5*a*, the first scan with FAD present was commenced at a potential of 0.250 V vs. NHE. The ac response shows a fairly broad peak, due to the pseudocapacity of the adsorbed electroactive material, and the double layer capacity on either side of the peak. At the start of the first negative sweep, the ac current is already lower than that of the supporting electrolyte alone, indicative of the onset of an adsorption process (34). The capacitance peak appears at a potential very close to the formal potential for FAD reduction, i.e. about −0.205 V vs. NHE. It will be shown below that the appearance of a single broad ac peak in the first few scans is indicative of Stage I of the adsorption of FAD.

It can be seen in Fig. 5*a* that the ac current obtained in the FAD-containing solution is closer to that for the buffer alone at potentials negative of the capacitance peak than at positive potentials. At pH = 7, the reduced form is expected to be partly anionic (1) and therefore it is likely that the negatively charged electrode would "destabilize" the anionic reduced form of the FAD layer.

On the first positive-going sweep in Fig. 5*a*, the ac peak appears as two smaller, but sharper ac peaks. Only one peak is seen at lower frequencies or if the solution is made substantially more conductive. After crossing these peaks, the current reaches its lowest value, before rising sharply at about +0.050 V. On the second cathodic sweep, the current drops sharply at about −0.030 V. After crossing the two peaks in this direction, the current remains low, increasing suddenly at about −0.550 V. Therefore, a type of capacitance "pit" or "well", also seen in the adsorption of nucleosides (35, 36), is observed between ca. −0.550 and ca. 0 V. The presence of this "pit" and the two sharp peaks is characteristic of "Stage II" of FAD adsorption. It is interesting to note that the centre of the capacitance "pit" is close to the pzc of Hg in phosphate solutions, i.e. about −0.200 V vs. NHE (21).

"Stage III" of FAD adsorption is observed after several hours of potential cycling over the range of potential in Fig. 5*a*. The ac response of this stage is shown in Fig. 6*a*, and it can be seen that now, the two ac peaks have again partly merged into one and that the capacitance "pit" has disappeared.

The development of Stages I to Stages III of FAD adsorption can also be followed by CV, as seen in Figs. 5*b* and 6*b*. It should be recalled that as s (used in the CV experiments) is 100 mV/s, much less time elapses per cycle as compared to a single cycle in the ac experiment. In the first few cycles of potential in Fig. 5*b*, a pair of broad peaks having a width at half height of ca. 70 mV (Peaks A_I and C_I, respectively) are seen. Both of these increase in magnitude with each cycle, and are centered near the expected potential for FAD reduction and oxidation. The charging current which flows on either side of the peaks decreases with continued cycling of the potential, consistent with the ac results of Fig. 5*a*. These broad peaks, A_I and C_I, are considered to depict "Stage I" of FAD adsorption. When a critical charge density of about 8 to 9 $\mu C/cm^2$ has passed, Stage I is complete and Stage II commences.

As seen in Fig. 5*b*, a sudden change in the appearance of the CV occurs as Stage II of FAD adsorption ensues. This is seen by the fact that within one or two sweeps of potential, and as the charge continues to increase, the cathodic peak (C_{II}) becomes sharp and narrow (width at half height about 40 mV) and a small, sharp shoulder ($A_{II,sh}$) appears on the positive side (at about −0.150 V) of the anodic peak. In addition, several small peaks appear at about +0.050 V (peak A′), at about −0.080 V (peak C′) and at about −0.530 V (peak C″), precisely the same potentials as where the capacitance "pit" is entered and exited in Fig. 5*a*. These peaks will be referred to as "capacitance peaks" here, as they depict the sudden changes in the double layer capacitance with potential, as seen clearly in the ac results of Figs. 5*a* and 6*a*.

"Stage III" of FAD adsorption occurs after long times of potential cycling between the extended potential limits of Figs. 5 and 6, and the CV response for "Stage III" is shown in Fig. 6*b*. Now, only a single broad pair of anodic and cathodic peaks (Peaks A_{III} and C_{III}) are observed, having a width at half height of about 70 mV. It should also be noted that the capacitance peaks A′, C′, and C″ are all now absent, consistent with the disappearance of the "pit" in Stage III in Fig. 6*a*. The relative narrowness of the peaks for Stage II as compared to Stages I and

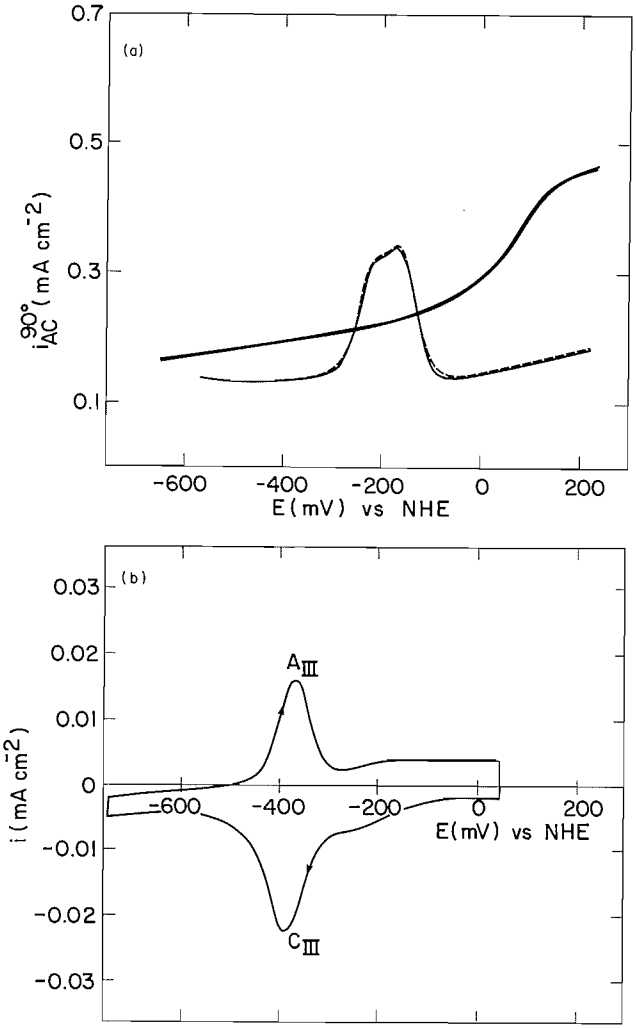

FIG. 6. Adsorption of FAD (Stage III) at the HMDE in 1.8×10^{-6} *M* FAD solution (pH = 7, 0.08 *M* phosphate buffer), after 1.5 h of continuous potential cycling to $E_- = -0.65$ V. (*a*) ac voltammogram where $\Delta E = 5$ mV, $\nu = 329$ Hz, $s = 5$ mV/s. (—) buffer solution only (no FAD); (—) cathodic sweep in FAD solution; (- - -) anodic sweep in FAD solution. (*b*) Cyclic voltammogram obtained immediately after recording the ac voltammogram in Fig. 6*a*; $s = 100$ mV/s.

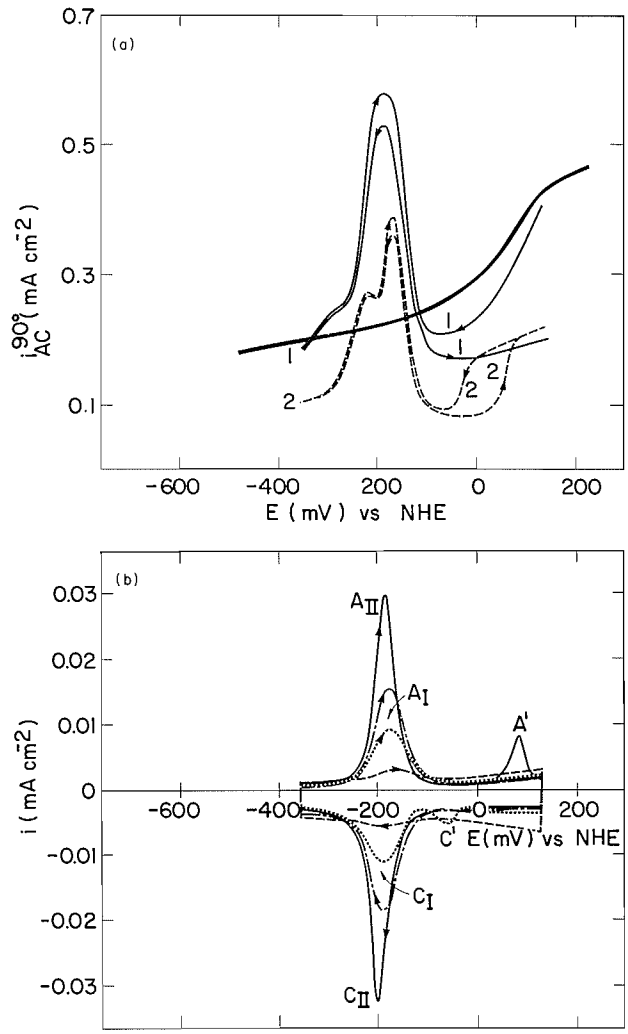

FIG. 7. Adsorption of FAD at a fresh HMDE over a less extended potential range than Fig. 5 ($E_- = -0.35$ V vs. -0.65 V); 1.8×10^{-6} *M* FAD solution (pH = 7). (*a*) ac voltammograms where $\Delta E = 5$ mV, $\nu = 329$ Hz, $s = 5$ mV/s. (—) buffer solution only (no FAD); (—) first sweep in FAD solution (curve 1); (- - -) third sweep in FAD solution (curve 2). (*b*) Cyclic voltammograms at $s = 100$ mV/s. (- - -) sweep no. 1; (···) sweep no. 10; (-·-) sweep no. 24; (—) sweep no. 38.

III is probably an indication of the presence of relatively strong lateral attractive forces within the adsorbed FAD layers in Stage II (37).

At higher FAD concentrations than 1.8×10^{-6} *M* (Figs. 5 and 6), the three stages of FAD deposition described above are also still seen, although in significantly fewer cycles, i.e. diffusion-controlled adsorption of FAD is observed. The i/E relationships for FAD adsorption are not in any way affected or controlled by the electrochemical technique utilized, e.g. CV, AC voltammetry or potential holding. However, the orientation of FAD on the electrode surface does depend strongly on time and on the potential.

(ii) Effect of potential limits

The effect of the potential limits on the mechanism of FAD adsorption can be seen most clearly from the results of the following two experiments. In Fig. 7, both the ac (Fig. 7*a*) and the CV (Fig. 7*b*) response is displayed for a fresh Hg drop when the negative voltage limit (E_-) is -0.350 V (rather than -0.650 V, as in Figs. 5 and 6), i.e. E_- is kept within the range of the capacitance "pit" during the adsorption of FAD. It is seen that when the transformation to Stage II commences, both the cathodic and anodic peaks become sharp and narrow (Fig. 7*b*), as opposed to the case when the potential is extended negatively outside of the "pit" in each scan (Fig. 5*b*) and the anodic peak remains broad. A further change observed in Fig. 7*b* vs. Fig. 5*b* is that the sharp shoulder ($A_{II,sh}$), seen previously at about -0.150 V at the positive side of A_I, now has only a transient existence. The effects shown in Fig. 7 are independent of whether or not the positive potential limit, E_+, is extended positively of the "pit".

The result of a second important experiment involving the effect of the potential limits is shown in Fig. 8. Here, Stage II of FAD adsorption has been reached after a number of cycles of potential (not shown in Fig. 8) in which E_- has been extended outside of the capacitance "pit" to -0.650 V, as in Figs. 5 and 6. The sharp cathodic peak (C_{II}), broad anodic peak (A_I), shoulder ($A_{II,sh}$), and the three capacitance peaks are all observed. By varying E_+ for each sweep as shown in Fig. 8, it is seen that when E_+ is kept negative of the potential of $A_{II,sh}$, the

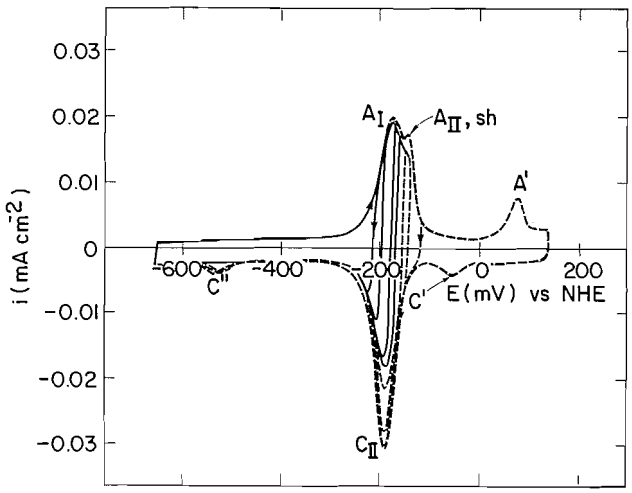

FIG. 8. Cyclic voltammograms of adsorbed FAD at HMDE after 24 cycles of potential at $s = 100$ mV/s; 1.8×10^{-6} M FAD solution (pH = 7). E_+ is increased with each potential cycle (nos. 1 to 8). Note that C'' appears only after cycle no. 5, when peak $A_{II,sh}$ has been reached.

principal cathodic peak is broad (C_I) and C'' is not observed. When E_+ reaches and crosses $A_{II,sh}$, the cathodic peak is narrower and C'' is clearly present, depicting Stage II of FAD adsorption.

These results show that if E_+ is not extended positively of the anodic shoulder, the "system" is not yet "within the capacitance pit". This confirms the ac results of Fig. 5*a*, which show that in Stage II, the capacitance drops as the two ac peaks are crossed when scanning positively. This experiment (Fig. 8) shows clearly that $A_{II,sh}$ is probably the indicator of this sudden change of the system capacitance as Stage I transforms to Stage II.

The results shown in Fig. 8 also give an indication of the kinetics of the oxidation and reduction of adsorbed FAD. When the potential is reversed within the range of peak A_{II}, the current immediately reverses in sign, indicative of a very fast process, particularly as the potential sweep rate is already reasonably high (100 mV/s). Also, the small peak separation indicates the rapid kinetics of adsorbed FAD oxidation and reduction. A more detailed kinetic discussion is presented later in this paper.

(iii) Surface formal potentials and charge densities – Stages I to III of FAD adsorption

Table 1 contains the surface formal potentials (E_f', the potential midway between the anodic and cathodic peaks) and the charge densities at the completion of each of the three stages of FAD adsorption described above. The table also lists the magnitude of the peak separation as well as the peak width at half height, all given at a potential sweep rate of 100 mV/s. It can be seen that Stages I and III, characterized by broad peaks having a width at half height of about 70 mV, have a E_f' about 20 mV more positive than does Stage II. Also, the formal potential of Stage II is closest to that obtained from the diffusion peaks (Fig. 2) at high FAD concentrations and low s. The peak separations given in Table 1 for the three stages of FAD adsorption also indicate that Stages I and III are similar, while Stage II is clearly different.

The variation of E_f' which occurs with time as the adsorption of FAD progresses through its stages points out clearly why it is difficult to reliably measure the formal potential (E_f) for FAD reduction and oxidation from the diffusion peaks (Fig. 2). At low s and high FAD concentrations, FAD adsorption would probably be complete by the time the reduction peak is reached in the first scan of potential. It is possible that Stage III would already be reached, which would lead to a positive shift of the measured E_f. At higher s, FAD adsorption would probably still be in Stage II, leading to a more negative measured E_f, while at very high s, Stage I could very well still be present in the first few sweeps. As the current response to adsorption would dominate at high s, a positive shift of the measured E_f might again be observed. This discussion stresses the difficulties associated with the measurement of a formal potential from a polarographic wave or a voltammetric peak when adsorption of the reactant and/or the product is occurring at the electrode surface as a function of time.

Significant disagreement exists in the literature regarding the quantity of RF and FMN which adsorbs at Hg electrodes and also how much charge constitutes a single layer of adsorbed flavin. For example, refs. 8 and 9 report that one molecule of adsorbed RF, with the isoalloxazine moiety parallel to the surface, would occupy an area of 150 Å^2, but observe 15 μC/cm^2 (212 Å^2) and 30 μC/cm^2 for one layer of oxidized RF and two layers of the reduced form of RF, respectively. Tedoradze *et al.* (10) have reported 22 μC/cm^2 (150 Å^2) as the charge for one monolayer of adsorbed oxidized RF and 30 μC/cm^2 for reduced RF on the electrode surface. The charge measured experimentally may depend on many variables such as solution pH, composition, and time of exposure of the electrode to the flavin solution. Some of these factors may account for the range in the reported values. Also, for bulkier molecules such as FAD, containing the phosphate and sugar groups of FMN, and also the rather large adenine group (Fig. 1), significantly more electrode surface area may be coupled per molecule, resulting in lower charge densities.

Overall, it appears that a value of 15 to 20 μC/cm^2 is a reasonable estimate of the charge equivalent to a single layer of flavin adsorbed with its isoalloxazine ring system flat on the electrode surface. Table 1 shows that Stage I of FAD adsorption is complete after 8 to 9 μC/cm^2 have passed, while Stages II and III involve a charge density of about 13 to 14 μC/cm^2. This latter charge density is consistent with the complete coverage of the Hg surface by FAD with its isoalloxazine system parallel to the electrode surface (the adenine ring can be assumed to lie above the surface, perhaps parallel to the isoalloxazine ring system, in a "stacked" configuration). The lower charge density observed for Stage I indicates a less tightly packed structure than for Stages II and III.

(iv) Kinetics of oxidation and reduction of adsorbed FAD

Figure 9*a* and *b* show plots of the peak current densities of Stages II and III as a function of potential sweep rate. In Fig. 9*a*, a linear relationship can be seen up to a sweep rate less than ca. 1 V/s, while Fig. 9*b* confirms that the deviation from linearity commences at a sweep rate greater than ca. 1 to 2 V/s. Although the charge density is the same for Stages II and III (Table 1), the currents are larger for Stage II (sharp, narrow peaks), as compared to Stage III (broad peaks), at any s.

The linear i_p/s relationship further confirms that Peaks II and III are due to the reduction/oxidation of adsorbed FAD. Because both the oxidized and the reduced form of FAD are strongly adsorbed on the Hg electrode surface, similar to the formation of a two-dimensional surface compound, it is probable that the reduction/oxidation reaction is activation controlled. Using CV, it is then anticipated that the i/E relationship should be exponential (38). However, the reaction

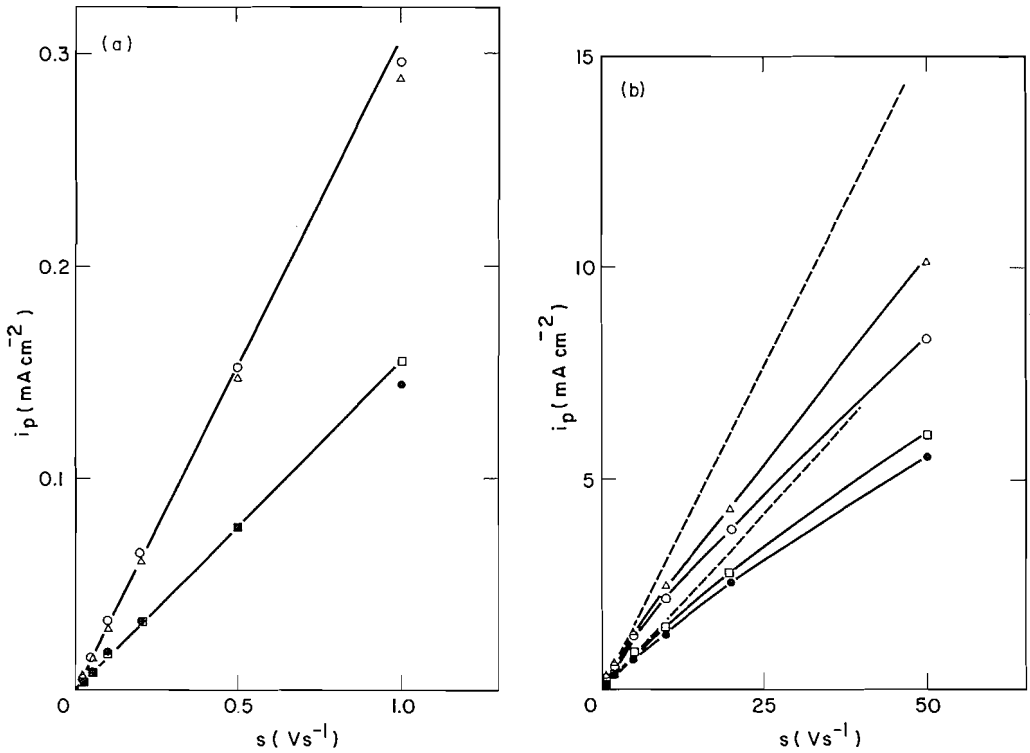

FIG. 9. Dependence of $i_{p,c}$ (○, ●) and $i_{p,a}$ (△, □) of adsorbed FAD on s; 1.8×10^{-6} M FAD solution (pH = 7); HMDE. Stage II (○, △); Stage III (●, □). (*a*) s less than 1 V/s. (*b*) s up to 50 V/s. The dashed lines represent the slope of the plots obtained at lower s (Fig. 9*a*).

rate will also depend on the number of available sites. Therefore, as the reaction progresses, e.g. cathodically, the tendency for the current to increase as the potential is made more negative will be offset by the decreasing number of reducible sites remaining. This then leads to a characteristic peak-shaped i/E response, such as seen in Figs. 5*b* and 6*b*. The same is true in the reverse (anodic) sweep.

As long as the ratio of i_p to s is constant (i.e. at a sweep rate less than 1 V/s in Fig. 9*a*), the reaction can be considered to be at equilibrium. Under these conditions, the peak potential should be constant and ΔE_p should be zero, as the concentration of oxidized and reduced species should adjust to the equilibrium values at each potential. As the sweep rate is increased, the reaction will become irreversible, as evidenced by the change of the slope of the i_p/s plot. By varying s over a reasonably wide range, the reversibility parameter, s_0, i.e. the point at which the reaction becomes irreversible, can be determined (39). s_0 is directly linked to the surface reaction standard rate constant, $k^{0'}$, according to eq. [3] (39):

$$[3] \quad k^{0'} = s_0 zF/2RT$$

where F, R, and T have their usual meaning, and z (= 2) is the number of electrons transferred per molecule of adsorbed species.

As is well known (39), the magnitude and shape of the current peaks should be independent of the concentration of reactants in solution when the surface reaction is activation controlled, and hence no bulk concentration terms appear in eq. [3]. Using an s_0 of 1 V/s, the surface standard rate constant is found to be 40 s^{-1}, which is indicative of a relatively fast surface reaction, similar to the rate of H^+ reduction at Pt electrodes in alkaline solutions (40).

Figure 10 shows a plot of ΔE_p vs. log s for Stages I to III. In this dilute FAD solution, there are no contributions from the reaction of FAD in solution, i.e. only adsorbed FAD is involved, as is seen by the constant charge for each Stage at all s. Contrary to the prediction above that ΔE_p should be equal to zero when the reaction is kinetically reversible (i.e. $s < 1$ V/s), the plot shows a peculiar rise in ΔE_p at $s < 0.5$ V/s, although it does show a sharp increase in ΔE_p at $s > 1$ V/s, at least for Stages II and III, which were examined in Fig. 9. Considering first the plot at high sweep rates, it is important to note that for Stage I, ΔE_p increases significantly only when $s > 10$ V/s, i.e. the reaction of FAD in Stage I is much faster than in the later stages. Stages II and III appear to behave similarly kinetically, apparently becoming kinetically irreversible at $s > 1$ V/s.

The unusual increase in ΔE_p at low sweep rates can only be understood by assuming that the oxidized and reduced forms of adsorbed FAD are thermodynamically different. This is consistent with a previous report regarding the lack of true reversibility seen in the diffusion waves for FAD in solutions of high FAD concentration (14). It is possible that this implies that at low sweep rates, there is adequate time for the conversion of FAD from its flat to its "butterfly" conformation as it is reduced, and vice versa, so that the oxidized and reduced forms are thermodynamically different (by 10 to 20 mV). At higher s, there may simply be too little time for this change to take place. It should be noted in Fig. 10 that this thermodynamic difference is more pronounced for Stage I than for Stages III and II.

It is also possible that the difference in peak potentials, and hence of E_f', at low s, depicts the fact that the reduced form of FAD is partly anionic, while the oxidized form is neutral, and that these two different chemical forms of FAD have somewhat different redox potentials. This would imply that at high sweep rates, both the oxidized and reduced forms of FAD would be anionic or both would be neutral.

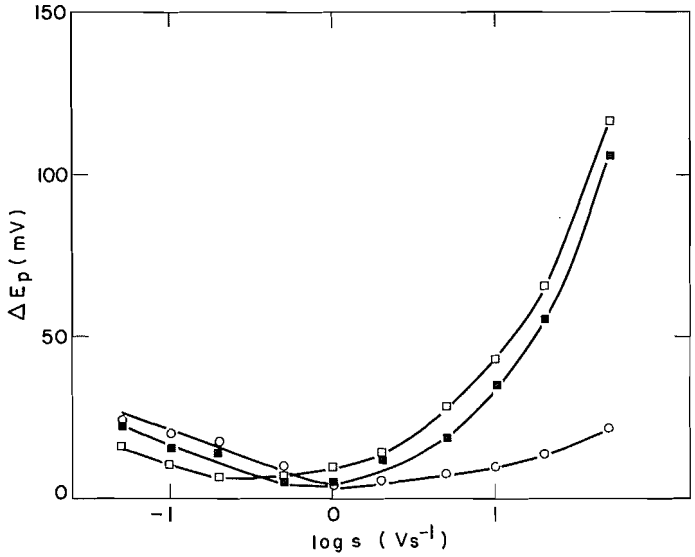

FIG. 10. ΔE_p vs. log s for adsorbed FAD; 1.8×10^{-6} M FAD solution (pH = 7). Stages of adsorption: (○) Stage I; (□) Stage II; (■) Stage III.

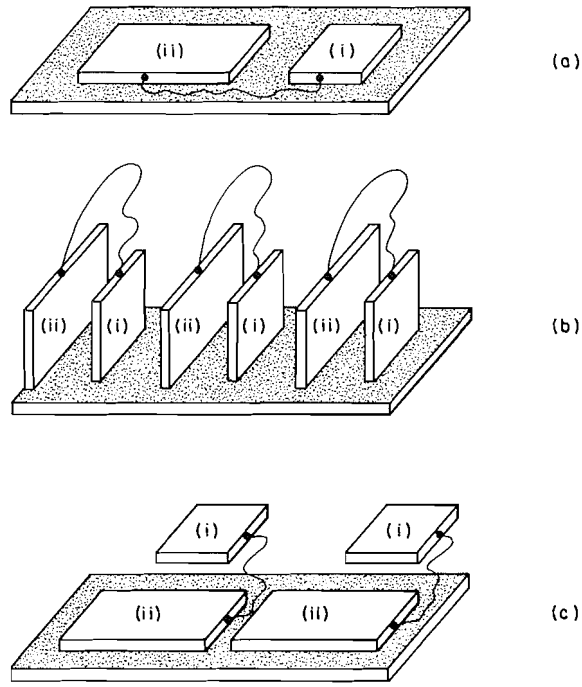

FIG. 11. Schematic of proposed orientation of adsorbed FAD at Hg electrodes, pH = 7; (*a*) Stage I; (*b*) Stage II; (*c*) Stage III. (*i*) Depicts the adenine group connected via the sugar–phosphato linkage to the isoalloxazine system (*ii*).

(v) Model of FAD adsorption at Hg electrodes

On the basis of all of the results presented above, the following model for the formation of an adsorbed FAD layer at Hg electrodes in pH 7 solutions is presented. When a fresh Hg drop is exposed to the FAD solution, FAD molecules adsorb as a function of time, as seen by the gradually increasing adsorption peaks with continuous potential sweeping (Fig. 5*b*). A time- and concentration-dependent loading of FAD on the surface of carbon electrodes has also been reported by Miyawaki and Wingard (19). It is proposed that the initial mode of adsorption (Peaks A_I/C_I) in the present work is such that the isoalloxazine moiety is approximately parallel to the electrode surface and the adenine groups are also on the Hg surface, as shown schematically in Fig. 11. This structure, having a large area per molecule (estimated to be about 400 Å^2), would be consistent with the relatively low charge densities of about 8 to 9 μC/cm^2 seen at this stage of deposition (Table 1). It should be noted that a "flat" orientation is actually more likely to be somewhat tilted, to enhance the overlap of the electron orbital on the N site on the isoalloxazine system with the Hg surface. A tilted structure has been suggested for the adsorption of pyridine on Pt electrode surfaces (41). The lack of significant lateral interactions between adjacent FAD molecules, due to the relatively loose structure of the layer and as the principal forces are probably between the Hg surface and the π electrons in the ring system would be consistent with the relatively broad nature of peaks A_I and C_I.

As the surface concentration of the loose FAD structure of Fig. 11*a* increases, a critical surface coverage is reached. Surface crowding then leads to a sudden change in orientation, represented by Stage II, for which it is suggested that the isoalloxazine ring system (and the adenine group) orients itself perpendicularly to the Hg surface, probably with the long end of the isoalloxazine moiety in contact with the electrode surface (Fig. 11*b*), similar to the vertical orientation assigned to adsorbed nucleosides when a "capacitance pit" is observed (35, 36). This suggestion is also supported by the larger surface coverage obtained in this orientation, as the π electrons of adjacent rings can overlap, leading to strong lateral interactions within the FAD layer. This leads to a more tightly packed layer, i.e. charge densities of about 13 to 14 μC/cm^2 and much sharper, narrower peaks (A_{II}, C_{II}) having a peak width of 35 to 40 mV (see Fig. 7). It should be pointed out that this perpendicular orientation is very stable when the potential is maintained within the region of the "capacitance pit", i.e. between $E = -0.550$ and 0.000 V. As long as the potential is kept within this range, the peaks will remain sharp and narrow and this orientation remains undisturbed.

When the potential is extended positively of the "pit", it is hypothesized that the now positively charged Hg surface provokes the isoalloxazine ring system to take on a parallel FAD orientation once again. This results in the observed increase in capacitance positive of the "pit". When the potential is scanned negatively, the FAD layer reorients itself again to the perpendicular orientation at $E = -0.050$ V (C′), resulting in a narrow cathodic peak (C_{II}) indicative of a perpendicular orientation with strong lateral interactions.

Figure 7 shows that when the potential is reversed during the cathodic sweep at a potential more positive than −0.550, i.e. inside the "pit", the FAD layer remains in the perpendicular orientation and a very sharp and narrow anodic peak, A_{II}, is observed. However, the extension of E_- to potentials negative of −0.550 V, i.e. out of the "pit", produces a broad anodic peak having a sharp shoulder in the next positive-going scan. On the basis of the above model, it appears that the reduced FAD layer, being at least partly anionic at pH 7, is not stable in the perpendicular orientation at negative electrode potentials and that the parallel orientation dominates at more negative potentials. This change to the parallel orientation at negative potentials is seen by the sudden increase of capacitance in Fig. 5*a* (i.e. C″ in Fig. 5*b*) at these potentials. The subsequent anodic sweep reveals a broad anodic peak, characteristic of a parallel orientation. However, as the FAD layer is oxidized,

it becomes neutral again, and therefore the perpendicular orientation is again favored. This transformation from parallel to perpendicular orientation occurs in the potential range of $A_{II,sh}$. This interpretation is consistent with the results of Fig. 5*a*, showing that the system is "inside the pit" after electro-oxidation, while it was "outside the pit" before the anodic reaction commenced.

After several hours of potential cycling over the full range of potential of Figs. 5 and 6, Stage III is reached. It is suggested that because of the broad nature of peaks A_{III} and C_{III} (Fig. 6*b*) and the similarity of these peaks to those seen in Stage I, the last stage of FAD adsorption again involves a parallel orientation of the isoalloxazine system to the Hg surface. This is supported by the absence of the capacitance peaks in CV experiments, i.e. the absence of the "pit". However, in order to make space for the equivalent of 13 $\mu C/cm^2$, the adenine group now positions itself directly above the isoalloxazene moiety in a "condensed structure" (Fig. 11*c*).

From Fig. 10, it is seen that the oxidation/reduction kinetics of adsorbed FAD are the most rapid for Stage I, when the principal interactions are thought to be between the isoalloxazine system and the Hg surface. For Stages II and III, when the strongest forces will be present between the isoalloxazine rings and the adenine system (Stage II and III) as well as between adjacent FAD molecules (Stage II), the redox reaction is somewhat slower.

Based on the above model (Fig. 11), it is also reasonable that Stage I, having no inter- or intra-molecular forces, other than to the electrode surface, would most readily take on the "butterfly" configuration in the reduced form at low s. This is consistent with the greatest thermodynamic difference being seen in Fig. 10 at low s for this stage, as compared to Stages II and III, which would be more constrained due to the presence of attractive forces between the isoalloxazine and adenine groups. Also, the observed negative shift of E_f' for Stage II vs. Stages I and III would be consistent with the predicted increase in the reducing power of the flavin, i.e. the negative shift of the redox potential, when the isoalloxazine ring system is held in the flat (vs. butterfly) orientation in the reduced state. This is more likely to be possible in Stage II than in the other Stages, as the strong lateral interactions between the FAD molecules (Fig. 11*c*) would tend to prevent any bending of the ring system during its oxidation and reduction.

Acknowledgements

Grateful acknowledgement is made to the Natural Sciences and Engineering Research Council of Canada for support of this work. Thanks are also extended to D. A. Armstrong for supplying the flavin salt and for numerous helpful discussions, and to Eileen Clarke for technical assistance.

1. G. Dryhurst, K. M. Kadish, F. Scheller, and F. Renneberg. *In* Biological electrochemistry. Vol. 1. Academic Press, Toronto. 1982. Chap. 7.
2. P. Hemmerich, C. Veeger, and H. C. S. Wood. Angew. Chem. Inter. Edit. **4**, 671 (1965).
3. B. Janik and P. J. Elving. Chem. Rev. **68**, 295 (1968).
4. T. C. Bruice. Prog. Bioinorg. Chem. **4**, 2 (1976).
5. B. Breyer and T. Biegler. J. Electroanal. Chem. **1**, 453 (1959/60).
6. B. Breyer and T. Biegler. Czech. Chem. Commun. **25**, 3348 (1960).
7. S. V. Tatwawadi and A. J. Bard. Anal. Chem. **36**, 2 (1964).
8. M. L. Foresti, F. Pergola, G. Aloisi, and R. Guidelli. J. Electroanal. Chem. **137**, 341 (1982).
9. M. L. Foresti, F. Pergola, G. Aloisi, and R. Guidelli. J. Electroanal. Chem. **137**, 355 (1982).
10. G. A. Tedoradze, E. Khmel'nitskaya, and Ya. M. Zolotovitskii. Sov. Electrochem. **3**, 200 (1967).
11. A. M. Hartley and G. S. Wilson. Anal. Chem. **38**, 681 (1966).
12. T. Kakutani, K. Kano, S. Ando, and M. Senda. Bull. Chem. Soc. Jpn. **54**, 884 (1981).
13. T. Kakutani, I. Katasho, and M. Senda. Bull. Chem. Soc. Jpn. **56**, 1761 (1983).
14. R. D. Braun. J. Electrochem. Soc. **124**, 1342 (1977).
15. O. Miyawaki and L. B. Wingard, Jr. Biotechnol. Bioeng. **26**, 1364 (1984).
16. L. Gorton and G. Johansson. J. Electroanal. Chem. **113**, 151 (1980).
17. L. B. Wingard, Jr. Trends Anal. Chem. **3**, 235 (1984).
18. O. Miyawaki and L. B. Wingard, Jr. Biochim. Biophys. Acta, **838**, 60 (1985).
19. O. Miyawaki and L. B. Wingard, Jr. Enzyme Eng. 7, Vol. **434**, 520 (1984).
20. K. Narasimham and L. Wingard, Jr. App. Biochem. Biotech. **11**, 221 (1985).
21. E. R. Gonzalez, A. Carubelli, and S. Srinivasan. Electrochim. Acta, **30**, 191 (1985).
22. A. J. Bard and L. R. Faulkner. Electrochemical Methods. John Wiley and Sons. 1980. pp. 218, 219, 522.
23. S. Van den Berghe-Snorek and M. T. Stankovich. J. Am. Chem. Soc. **106**, 3683 (1984).
24. R. F. Anderson. Biochim. Biophys. Acta, **722**, 158 (1983).
25. C. Walsh, J. Fisher, R. Spencer, D. W. Graham, W. T. Ashton, J. E. Brown, R. D. Brown, and E. F. Rogers. Biochemistry, **17**, 1942 (1978).
26. Y. Asahi. J. Pharm. Soc. Jpn. **76**, 378 (1956).
27. O. S. Ksenzhek, S. A. Petrova, and I. D. Pinielle. Sov. Electrochem. **11**, 1603 (1975).
28. Z. Brdicka. Zeit. Elektrochem. **48**, 278 (1942).
29. B. Ke. Arch. Biochem. Biophys. **68**, 330 (1957).
30. M. T. Stankovich. Anal. Biochem. **109**, 295 (1980).
31. M. J. Clarke, M. G. Dowling, A. R. Garafalo, and T. F. Brennan. J. Am. Chem. Soc. **101**, 223 (1979).
32. M. J. Clarke and M. G. Dowling. Inorg. Chem. **20**, 3506 (1981).
33. M. G. Dowling and M. J. Clarke. Inorg. Chim. Acta, **78**, 153 (1983).
34. B. B. Damaskin, O. A. Petrii, and V. V. Batrakov. *In* Adsorption of organic compounds on electrodes. Plenum Press, New York. 1971.
35. W. T. Bresnahan, J. Moiroux, Z. Samec, and P. J. Elving. Bioelectrochem. Bioeng. **7**, 125 (1980).
36. V. Vetterl, K. Kovarikova, and R. Zaludova. Bioelectrochem. Bioeng. **4**, 389 (1977).
37. E. Laviron. Electroanalytical chemistry. Vol. 12. *Edited by* Allen J. Bard. Marcel Dekker Inc. 1982. p. 53.
38. H. Angerstein-Kozlowska, J. Klinger, and B. E. Conway. J. Electroanal. Chem. **75**, 45 (1977).
39. H. Angerstein-Kozlowska and B. E. Conway. J. Electroanal. Chem. **95**, 1 (1979).
40. H. Angerstein-Kozlowska and B. E. Conway. J. Electroanal. Chem. **87**, 321 (1978).
41. A. L. Johnson and E. L. Muetterties. J. Phys. Chem. **89**, 4071 (1985).